Targeting ETHE1 inhibits tumorigenesis *in vitro* and *in vivo* by preventing aerobic glycolysis in gastric adenocarcinoma cells

FANGFEI LI, XUAN DU, MEI HAN, XIAOYING FENG and CHUNMENG JIANG

Department of Gastroenterology, The Second Hospital of Dalian Medical University, Dalian, Liaoning 116027, P.R. China

Received August 21, 2024; Accepted January 20, 2025

DOI: 10.3892/ol.2025.15032

Abstract. Gastric adenocarcinoma (GAC) is a prevalent form of cancer that frequently displays abnormal metabolism characterized by increased aerobic glycolysis. Therefore, inhibition of glycolysis may exhibit therapeutic potential for the management of advanced or recurrent gastric cancer. Analysis of ethylmalonic encephalopathy protein 1 (ETHE1) expression levels in 30 pairs of cancerous and paracancerous tissues, and 50 tumor tissue sections collected from patients with GAC revealed that ETHE1 expression was upregulated in cancerous tissues compared with in paracancerous tissues. Advanced tumor stage, lymph node metastasis and Tumor-Node-Metastasis stage were associated with high ETHE1 expression. Knockdown of ETHE1 expression in GAC cells resulted in a significant inhibition of cell proliferation and in cell cycle arrest, accompanied by downregulated levels of cyclin D1 and cyclin-dependent kinase 4. ETHE1 knockdown also resulted in increased apoptosis of GAC cells, and increased caspase-3 and caspase-9 activity. Additionally, the expression levels of proteins associated with aerobic glycolysis were downregulated following ETHE1 knockdown, which may reduce glucose consumption, lactic acid production and ATP levels. In the *in vivo* experiments, suppressed tumor growth and increased tumor cell apoptosis were observed in the xenograft tumor model in animals injected with ETHE1-knockdown GAC cells. In summary, knockdown of ETHE1 inhibited aerobic glycolysis, promoted apoptosis and inhibited tumor cell proliferation in GAC cells. These results highlight ETHE1 as a promising molecular target for the treatment of GAC potentially using an adjuvant to target it, offering a novel approach in the exploration of targeted therapeutic drugs for GAC.

Correspondence to: Professor Chunmeng Jiang or Professor Xiaoying Feng, Department of Gastroenterology, The Second Hospital of Dalian Medical University, 467 Zhongshan Road, Dalian, Liaoning 116027, P.R. China
E-mail: chunmengjiang@dmu.edu.cn
E-mail: fengxiaoying39@126.com

Key words: gastric adenocarcinoma, ethylmalonic encephalopathy protein 1, aerobic glycolysis, tumor growth, apoptosis

Introduction

Gastric cancer (GC) is one of the most common malignancies. Data from the International Agency for Research on Cancer indicated that in 2020, the global incidence of GC accounted for 5.6% of all cancer cases and 7.7% of all cancer deaths, and it is the third leading cause of cancer-related death worldwide (1). The most common subtype of GC is gastric adenocarcinoma (GAC) (2). At present, surgical resection, chemotherapy and radiotherapy are the primary treatments for GC; however, there is a need for more effective treatments for advanced or recurrent GC (3). Thus, the use of drugs that target key disease-causing molecules is an increasingly attractive therapeutic approach.

Accelerated energy metabolism is one of the characteristics of cancer cells, which typically relies on increased glucose consumption and accelerated aerobic glycolysis (4). Aerobic glycolysis refers to the phenomenon in which tumor cells metabolize glucose through glycolysis in an oxygen-rich environment, resulting in the production of a significant amount of lactic acid. This phenomenon is referred to as the Warburg effect (5), which has been hypothesized to be an adaptive mechanism that supports the uncontrolled proliferation of tumor cells. In this process, tumor cells rely on increased glucose consumption as the carbon source for cell proliferation (6). In addition, the lactic acid produced by this process is involved in various mechanisms of tumor formation. It reduces T-cell activity and inhibits the cytotoxicity of natural killer (NK) cells (7). Furthermore, it promotes tumor angiogenesis and provides a suitable microenvironment for tumor development (8). Abnormal glucose metabolism can typically be observed in GC tissue (9,10), and targeted inhibition of glycolysis has demonstrated a positive effect in inhibiting the progress of GC (11,12). Therefore, aerobic glycolysis may be an important therapeutic target for GAC.

Ethylmalonic encephalopathy protein 1 (ETHE1) is a hydrogen sulfide catabolic enzyme, the expression of which is widely distributed in eukaryotic animal tissues (13). It has been reported that ETHE1 expression is upregulated in triple-negative breast cancer where it increases the malignant behaviors of tumor cells (14). Furthermore, overexpression of ETHE1 has been shown to promote aerobic glycolysis and promote the progression of colorectal cancer (15). However, to the best of our knowledge, the role of ETHE1 in GAC has not yet been determined. ETHE1 has been specifically implicated

in energy metabolism and mitochondrial function, which involves the glycolytic pathway (16,17). Gene expression analysis of GC samples has shown that ETHE1 is upregulated in GC tissues, where it may be involved in tumor invasion, metastasis and carcinogenesis (18,19). Based on these previous findings, it was hypothesized that ETHE1 may be involved in aerobic glycolysis in GAC. The present study assessed the association between ETHE1 expression levels in clinical tissue samples and GAC staging. In addition, the regulatory effects of ETHE1 on GAC cell proliferation and glycolysis were assessed by knocking down ETHE1 expression.

Materials and methods

Bioinformatics analysis. For pan-cancer analysis, the expression data of ETHE1 in clinical samples from The Cancer Genome Atlas (TCGA) and Genotype-Tissue Expression (GTEx) datasets were downloaded from the University of California, Santa Cruz database (http://xena.ucsc.edu/); the details are shown in Table SI. The difference in ETHE1 expression in tumor and normal tissues was analyzed using a non-parametric test (Wilcoxon rank-sum test). The immunohistochemical results of ETHE1 in GC tissues and normal tissues from healthy controls were analyzed using the Human Protein Atlas (HPA) database (https://www.proteinatlas.org/). Survival analysis was performed based on the expression data of ETHE1 in patients with stomach adenocarcinoma (STAD) from the data obtained from TCGA using Kaplan-Meier analysis. Survival analysis results and survival plots were generated using Gene Expression Profiling Interactive Analysis (GEPIA; http://gepia.cancer-pku.cn/) (20), and the high and low cutoff values were set to 50%. The Spearman correlation analysis was performed to determine the correlation between ETHE1 expression in STAD and immunomodulator expression using the TISIDB database (http://cis.hku.hk/TISIDB/index.php) (21). ETHE1 expression in regulatory T cells (Tregs) and M2 macrophages in STAD tumor tissues and paracancerous tissues were analyzed using GEPIA based on the data from TCGA.

Patients and tissue samples. A total of 30 pairs of fresh cancerous and paracancerous tissues from 30 patients with GAC who underwent surgical resection at The Second Hospital of Dalian Medical University (Dalian, China) were collected between April 15, 2023 and October 30, 2023. The patients were aged 39-85 (mean age, 65.7 years), 80% were men and 20% were women. These fresh tissues were used to detect ETHE1 expression. In addition, the clinical characteristics of 50 patients with GAC who had not received preoperative chemotherapy or radiotherapy were collected from The Second Hospital of Dalian Medical University between April 15, 2023 and October 30, 2023. These patients were aged 47-85 year (mean age, 65.2 years), 78% were men and 22% were women. The paraffin-embedded cancerous tissue samples of the 50 patients were used to detect ETHE1 expression. The association between ETHE1 expression and the clinical characteristics of patients with GAC was analyzed using a Yates's corrected χ^2 test or Fisher's exact test. All of the specimens were collected under a protocol approved by the Ethics Committee of The Second Hospital of Dalian Medical University (2023; approval no. 136). Each patient provided written informed consent, and the study was performed in accordance with The Declaration of Helsinki.

Cell lines. All cell lines were purchased from iCell Bioscience Inc. The human GAC AGS cell line was cultured in Ham's F-12K medium (Wuhan Servicebio Technology Co., Ltd.) supplemented with 10% FBS (Zhejiang Tianhang Biotechnology Co., Ltd.), 1% penicillin and 1% streptomycin. GES-1, SNU-1, NCI-N87 and MKN-45 cells were cultured in RPMI-1640 medium (Beijing Solarbio Science & Technology Co., Ltd.) supplemented with 10% FBS. All of the cells were maintained at 37˚C in a humidified incubator supplied with 5% CO_2 air.

Cell infection. The 2nd lentiviral system was used to infect the NCI-N87 and MKN-45 cells. Short hairpin (sh)RNA constructs were synthesized by General Biotech (Anhui) Co., Ltd. and were cloned into the pLKO.1-EGFP-puro vector (Fenghbio). The sequences of the shRNAs were: ETHE1-shRNA (708-728; $sh^{708-728}$), 5'-ccgGATAGACTTTGCTGTTCCAGCttcaagagaGCTGGAACAGCAAAGTCTATCtttttt-3', ETHE1-shRNA (557-577; $sh^{557-577}$), 5'-ccgCAGGAGACTGTCTGATCTACCttcaagagaGGTAGATCAGACAGTCTCCTGtttttt-3', and negative control (NC)-shRNA 5'-ccgTTCTCCGAACGTGTCACGTttcaagagaACGTGACACGTTCGGAGAAttttttt-3'. The numbers 708-728 and 557-577 represent the target sequence position of the shRNA. The uppercase letters represent ETHE1-specific sequences, and the lowercase letters represent hairpin sequences. The ETHE1-targeted interference vectors (14 μg), packaging plasmids (10.5 μg) and envelope plasmids (3.5 μg) were co-transfected into 293T cells (iCell Bioscience Inc.) using Lipofectamine® 3000 (Invitrogen; Thermo Fisher Scientific, Inc.) to produce lentiviral particles that were used to infect cells. The 293T cells were cultured at 37˚C with 5% CO_2, and 48 h post-transfection with the plasmid vectors, the supernatant containing lentiviral particles was collected. Subsequently, 48 h after transduction, stably infected cells were screened, and subsequent experiments were performed 5 days later. In detail, the NCI-N87 [multiplicity of infection (MOI)=10] and MKN-45 (MOI=20) cells were seeded in 6-well plates and cultured in media containing lentiviral particles ($2x10^8$ TU/ml; NCI-N87 cell, 10 μl/well; MKN-45 cell, 20 μl/well) at 37˚C and 5% CO_2 for 24 h, the media were then replaced with fresh media and the cells were cultured for a further 24 h. Control cells were transfected with a lentivirus carrying a shRNA that lacked a specific target sequence (NC-shRNA). The cells were cultured in complete culture medium containing puromycin (NCI-N87, 1.5 μg/ml; MKN-45, 2.5 μg/ml) for 5 days to screen for stably infected cells. The stably infected NCI-N87 and MKN-45 cells were maintained in media containing 0.3 and 0.5 μg/ml puromycin, respectively.

Tumor xenograft model. A total of 10 male BALB/c nude mice (age, 6 weeks; body weight, 17-19 g) supplied by Beijing Vital River Laboratory Animal Technology Co., Ltd. The mice were randomly divided into the following two groups: Control and $sh^{708-728}$ (n=5/group). The mice were reared under a 12-h light/dark cycle, at a temperature of 22±1˚C and a humidity

level of 45-55%. The mice were allowed to eat and drink freely, and their health and behavior were monitored every 4-6 h. After 1 week of adaptive feeding, the mice were subcutaneously injected with the NCI-N87 cell line ($2x10^6$ cells; 0.2 ml/mouse). The $sh^{708-728}$ group received ETHE1-knockdown NCI-N87 cells, while the control group was injected with cells infected with the NC-shRNA lentivirus. Tumor volume was measured every 3 days following tumor formation. At the end of the experiment (day 25), mice were euthanized using CO_2 with a volume displacement rate of 50%/min, followed by cervical dislocation. Tumor tissues were collected for subsequent experiments.

For animal welfare reasons, the animals were kept in a constant temperature and humidity environment, and the experimental procedures were carried out by skilled experimenters to reduce the temporary tension and pain caused by subcutaneous injection. Based on the National Institutes of Health Guidelines for Endpoints in Animal Study Proposals (22), humane endpoints in the study included tumors growing to >15 mm in diameter, and ulceration or infection of the growth site. A total of 10 animals were used in the study, all of which were euthanized at the end of the experiment. No animals were found dead during the experiment. All the animal experiments were approved by the Animal Care and Welfare Committee of Dalian Medical University (approval no. AEE23074).

Reverse transcription-quantitative polymerase chain reaction (RT-qPCR). Total RNA from clinical samples or cells (NCI-N87 and MKN-45) were extracted using TRIpure lysis buffer (Bioteke Corporation) and cDNA was obtained by RT. The mixture including oligo $(dT)_{15}$ (Takara Biotechnology Co., Ltd.) and random primers synthesized by General Biotech (Anhui) Co., Ltd. was heated at 70˚C for 5 min, and was cooled on ice for 2 min. Subsequently, dNTP (Beijing Solarbio Science & Technology Co., Ltd.), buffer (Beyotime Institute of Biotechnology), RNase inhibitor (Sangon Biotech Co., Ltd.) and reverse transcriptase (Beyotime Institute of Biotechnology) were added to the mixture, which was heated at 25˚C for 10 min and 42˚C for 50 min, before the reaction was terminated by heating at the mixture at 80˚C for 10 min. qPCR was performed using SYBR GREEN (Beijing Solarbio Science & Technology Co., Ltd.) and 2X Taq PCR MasterMix (Beijing Solarbio Science & Technology Co., Ltd.) on a fluorescence quantifier (Exicycler™ 96, Bioneer Corporation). The qPCR thermocycling conditions were as follows: Initial denaturation at 95˚C for 5 min(), followed by 40 cycles at 95˚C for 10 sec (denaturation), 60˚C for 10 sec (annealing) and 72˚C for 15 sec (extension). The mRNA levels were quantified using the $2^{-\Delta\Delta Cq(Cq\ test-Cq\ reference)}$ formula (23). The sequences of the primers used were: ETHE1 forward, 5'-GTCATCTCC CGCCTTAGTG-3' and reverse, 5'-CGGATCAACAGGGCA TCT-3'; and GAPDH forward, 5'-GACCTGACCTGCCGT CTAG-3' and reverse, 5'-AGGAGTGGGTGTCGCTGT-3'. GAPDH was used as the internal control gene.

Western blot analysis. Total protein was extracted from clinical samples or cells (NCI-N87 and MKN-45) using RIPA lysis buffer (Beijing Solarbio Science & Technology Co., Ltd.), and the protein concentration was determined using a BCA protein concentration assay kit (Beijing Solarbio Science & Technology Co., Ltd.). Protein samples (20 μg) were loaded onto SDS-gels (5% stacking gel, 8-12% separation gel), resolved using SDS-PAGE and transferred to PVDF membranes (MilliporeSigma). The membranes were then blocked using a blocking solution (cat. no. SW3010; Beijing Solarbio Science & Technology Co., Ltd.) for 1 h and washed. Subsequently, the membranes were incubated with primary antibodies (1:1,000) overnight at 4˚C and with the secondary antibody (1:3,000) for 1 h at room temperature. After washing, enhanced chemiluminescence solution (Beijing Solarbio Science & Technology Co., Ltd.) was added to the membranes, which were exposed in a dark room and imaged using a gel imaging system (WD-9413B; Beijing Liuyi Biotechnology Co., Ltd.). The antibodies used in the present study are listed in Table I.

Immunohistochemistry. Tumor tissue was fixed in 4% paraformaldehyde overnight at room temperature, and dehydrated in an increasing series of ethanol concentrations (70, 80, 90 and 100%). Dehydrated tissues were permeabilized in xylene and embedded in paraffin. Paraffin-embedded tissues were cut into 5-μm sections, which were immersed in xylene, rehydrated in a descending series of ethanol concentrations (95, 85 and 75%), boiled in antigen retrieval solution (Beyotime Institute of Biotechnology) for 10 min, washed in PBS buffer, and incubated with 3% H_2O_2 (Sinopharm Chemical Reagent Co., Ltd.) for 15 min at room temperature to inactivate endogenous peroxidase activity. Subsequently, the sections were blocked with 1% BSA (Sangon Biotech Co., Ltd.) for 15 min at room temperature. After washing, the sections were incubated with primary antibodies (Ki67 antibody, 1:1,000; ETHE1 antibody, 1:200) at 4˚C overnight, followed by incubation with a horseradish peroxidase-conjugated secondary antibody (1:500) for 1 h at room temperature. The protein expression was visualized using DAB (Fuzhou Maixin Biotechnology Development Co., Ltd.). Finally, sections were counterstained with hematoxylin (Beijing Solarbio Science & Technology Co., Ltd.) and images were captured using a light micrograph system (DP73; Olympus Corporation). Antibody details are provided in Table I.

Cell viability assay. Cells (NCI-N87 and MKN-45) were seeded in 96-well plates ($5x10^3$ cells/well) and cell viability was assessed using a Cell Counting Kit-8 cell proliferation assay kit (Nanjing KeyGen Biotech Co., Ltd.) according to the manufacturer's protocol. Cells were incubated with CCK-8 reagent for 2 h at 37˚C. The absorbance was measured at 450 nm using a microplate reader (800TS; BioTek; Agilent Technologies, Inc.).

EdU staining. Cells (NCI-N87 and MKN-45) were stained using a kFluor488 Click-iT EdU imaging assay kit (Nanjing KeyGen Biotech Co., Ltd.) according to the manufacturer's protocol. Briefly, virally infected cells were incubated with EdU for 2 h at 37˚C, fixed with 4% paraformaldehyde for 15 min at room temperature, and treated with the Click-iT reaction solution in the dark for 30 min at room temperature. Nuclei were counterstained with DAPI for 5 min at room temperature. Images were captured using a fluorescence microscope (IX53; Olympus Corporation).

Table I. Antibody information.

A, Western blotting

Antibody name	Provider	Cat. no.
ETHE1 antibody	ABclonal Biotech Co., Ltd.	A10142
Cyclin D1 antibody	ABclonal Biotech Co., Ltd.	A19038
Cyclin-dependent kinase 4 antibody	ABclonal Biotech Co., Ltd.	A16813
Glucose transporter type 1 antibody	ABclonal Biotech Co., Ltd.	A6982
Lactate dehydrogenase A antibody	ABclonal Biotech Co., Ltd.	A1146
Hexokinase 2 antibody	ABclonal Biotech Co., Ltd.	A0994
Pyruvate kinase isozyme type M2 antibody	ABclonal Biotech Co., Ltd.	A20991
GAPDH	Proteintech Group, Inc.	60004-1-Ig
Goat Anti-Rabbit IgG-HRP	Beijing Solarbio Science & Technology Co., Ltd.	SE134
Goat Anti-Mouse IgG-HRP	Beijing Solarbio Science & Technology Co., Ltd.	SE131

B, Immunohistochemistry

Antibody name	Provider	Cat. no.
Ki67 antibody	Proteintech Group, Inc.	27309-1-AP
ETHE1 antibody	Abcam	ab174302
Goat Anti-Rabbit IgG-HRP	Thermo Fisher Scientific, Inc.	31460

Flow cytometry. Cell cycle distribution and apoptosis were analyzed using a flow cytometer (NovoCyte-D2060R; Agilent Technologies, Inc.), and a Cell Cycle and Apoptosis Analysis Kit (BioSharp Life Sciences) or an Annexin V-APC/PI double staining apoptosis detection kit (Nanjing KeyGen Biotech Co., Ltd.), respectively, according to the manufacturers' protocols. Briefly, cells (NCI-N87 and MKN-45) were incubated in PI/RNase A solution in the dark for 30 min at room temperature, and then the cell cycle distribution was measured. In addition, the cells were incubated with 5-μl Annexin V-APC and 5 μl PI dye in the dark for 10 min at room temperature, and apoptosis was detected. Analysis was conducted using NovoExpress software (version 1.5.6; Agilent Technologies, Inc.).

TUNEL assay. The TUNEL assay was used to detect apoptosis. Cells (NCI-N87 and MKN-45) grown on glass coverslips were fixed with 4% paraformaldehyde for 10 min at room temperature and were then permeabilized using 0.1% Triton X-100 for 15 min at room temperature. Fluorescent labeling was performed using an In Situ Cell Death Detection Kit (Roche Diagnostics) according to the manufacturer's protocol. The cells were incubated with TUNEL reaction liquid for 1 h at 37˚C. For tissues, they were embedded in paraffin and cut into 5-μm sections. The sections were dewaxed, permeabilized and then labeled. The nuclei were counterstained with DAPI (Shanghai Aladdin Biochemical Technology Co., Ltd.) for 5 min at room temperature. The sections were sealed using antifading mounting medium (Beijing Solarbio Science & Technology Co., Ltd.) and the images of the sections were captured using a fluorescence micrograph system (three fields/sample).

Detection of caspase-3 and caspase-9 activity. Caspase-3 and caspase-9 activities in the NCI-N87 and MKN-45 cell lines were assessed using a caspase-3 activity assay kit (cat. no. C1116; Beyotime Institute of Biotechnology) and caspase-9 activity assay kit (cat. no. C1158; Beyotime Institute of Biotechnology), respectively, according to the manufacturer's protocol. Total protein was extracted using the lysis buffer provided by the kits. A Bradford protein concentration assay kit (Beyotime Institute of Biotechnology) was used to determine the total protein concentration, which was used to normalize the data. Caspase-3 and caspase-9 activity were assessed based on the concentration of the product of pNA, which is catalyzed by both caspase-3 and caspase-9. The absorbance of catalytic products was measured at 405 nm using a microplate reader (800TS).

Detection of markers of glycolysis. A glucose assay kit (cat. no. F006; Nanjing Jiancheng Bioengineering Institute), lactic acid assay kit (cat. no. A019; Nanjing Jiancheng Bioengineering Institute) and ATP assay kit (cat. no. S0026; Beyotime Institute of Biotechnology) were used to measure glucose consumption, lactate production and ATP content, respectively. The cells (NCI-N87 and MKN-45 cell lines) were lysed using ultrasonic processing (300 W, 3 sec, interval time 25 sec, 5 cycles) and a BCA protein concentration assay kit (Beyotime Institute of Biotechnology) was used to detect total protein concentration, which was used to normalize the data.

Statistical analysis. The *in vitro* experiments were repeated three times. Data are presented as the mean ± SD. Statistical analyses were performed using GraphPad Prism version 9.5.0 (Dotmatics). A two-tailed unpaired Student's t-test or one-way ANOVA followed by a Tukey's post hoc test was used to

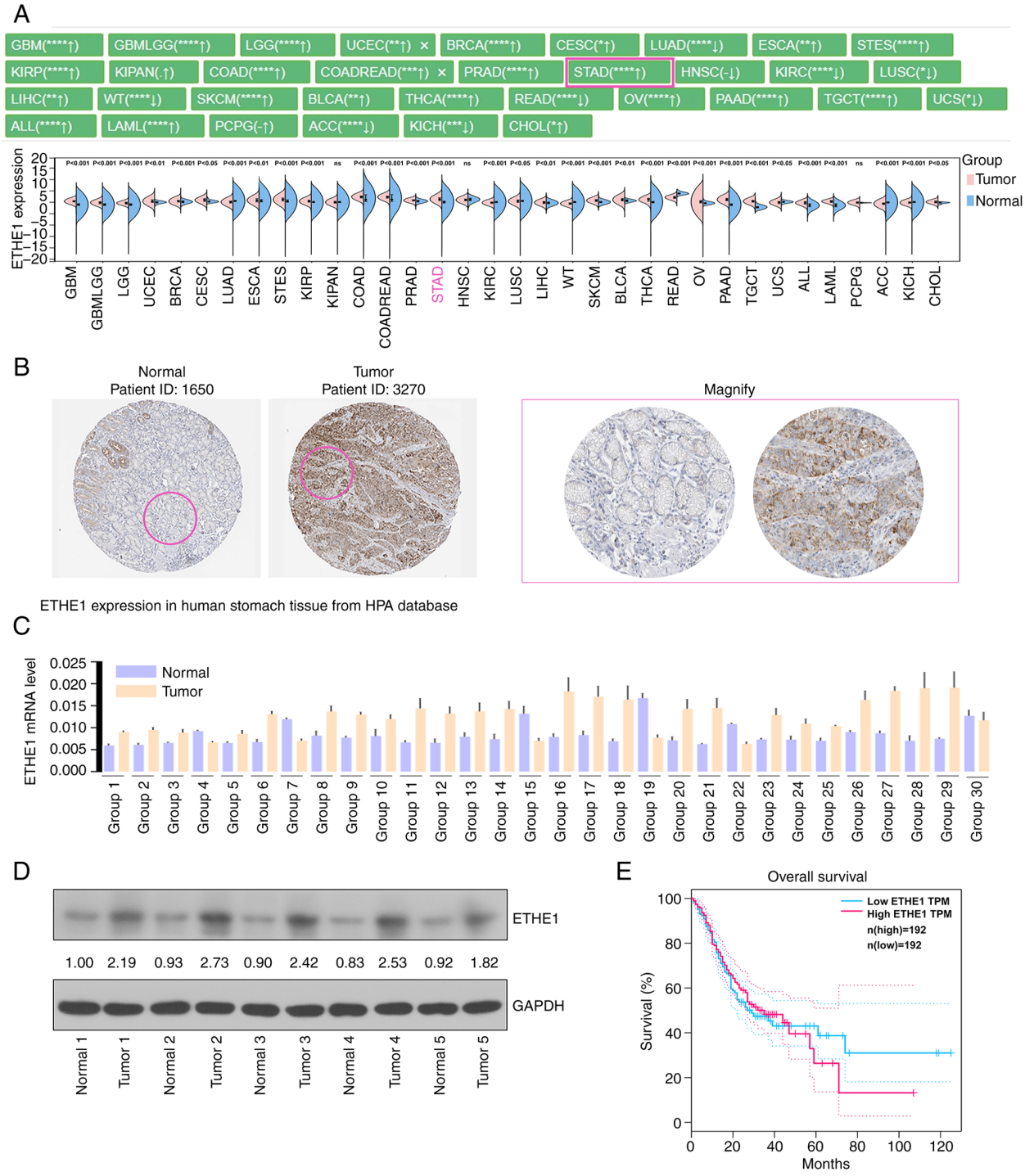

Figure 1. Analysis of ETHE1 expression in clinical samples. (A) ETHE1 expression in various types of cancer was analyzed based on TCGA and Genotype-Tissue Expression databases. (B) Immunohistochemical images of ETHE1 expression in normal gastric tissue and gastric cancer tissue were obtained from the Human Protein Atlas database. ETHEI expression in GAC and paracancerous tissues was detected using (C) reverse transcription-quantitative PCR and (D) western blotting. (E) Survival analysis of ETHE1 expression in STAD was conducted based on TCGA data. *P<0.05, **P<0.01, ***P<0.001, ****P<0.0001. ETHEI, ethylmalonic encephalopathy protein 1; GAC, gastric adenocarcinoma; STAD, stomach adenocarcinoma; TCGA, The Cancer Genome Atlas; ns, not significant.

analyze the differences between independent groups. P<0.05 was considered to indicate a statistically significant difference.

Results

ETHE1 expression is upregulated in GAC tissues and cells. Pan-cancer analysis showed that ETHE1 was differentially expressed in multiple types of cancer, such as STAD. Notably, the expression of ETHE1 in STAD samples was significantly higher than that in healthy control samples (Fig. 1A). Furthermore, the immunohistochemical results of ETHE1 in GC and normal tissues were analyzed using the HPA database, and ETHE1 expression was upregulated in tumor tissues (Fig. 1B). The present study detected

Table II. Correlation between ETHE1 expression levels and the clinicopathological characteristics of patients with GAC.

Parameter	Cases	ETHE1 expression		P-value
		Low (<Median[a])	High (≥Median[a])	
Sex				0.267
Male	39	6	33	
Female	11	4	7	
Age				0.813
≤60 years	14	3	11	
>60 years	36	7	29	
T stage				3.71074×10^{-5}
T1-T2	5	5	0	
T3-T4	45	5	40	
N stage				0.032
N0	7	4	3	
N1	43	6	37	
M stage				>0.99
M0	48	10	38	
M1	2	0	2	
TNM stage				0.033
I-II	18	7	11	
III-IV	32	3	29	
Histopathological grade				>0.99
G1	1	1	0	
G2-G3	49	9	40	
Tumor size				0.126
≤3 cm	13	5	8	
>3 cm	37	5	32	
Tumor number				>0.99
Unifocal	48	10	38	
Multifocal	2	0	2	

[a]Median value, 4. TNM, Tumor-Node-Metastasis.

the expression levels of ETHE1 in 30 pairs of GC tissues and paracancerous tissues. Analysis showed that ETHE1 expression was generally higher in cancerous tissues than that in paracancerous tissues (Fig. 1C and D). Additionally, upregulated expression of ETHE1 was associated with a worse survival time (Fig. 1E). The association between ETHE1 expression levels and clinicopathological characteristics are shown in Table II. A higher tumor stage, lymph node metastasis or higher Tumor-Node-Metastasis (TNM) stage was associated with higher expression of ETHE1, indicating a potential link between ETHE1 and GAC. Representative immunohistochemical images of high and low ETHE1 expression in GAC tissues are shown in Fig. 2A. Furthermore, the expression levels of ETHE1 in GAC cell lines were higher than those in the normal gastric mucosa cell line GES-1, and the expression levels were relatively higher in NCI-N87 and MKN-45 cells than in AGS and SNU-1 cell lines (Fig. 2B and C). Therefore, these two cell lines were selected for further study.

ETHE1 knockdown inhibits GAC cell proliferation. As shown in Fig. 3A, compared with in the control group, intracellular ETHE1 expression was successfully knocked down ~4-fold. Cell proliferation was inhibited following lentiviral infection for 48 h (Fig. 3B). Furthermore, the number of EdU-positive cells was reduced, indicating that GAC cell proliferation was reduced following ETHE1 knockdown (Fig. 3C). Cell cycle distribution was measured using flow cytometry. As shown in Fig. 3D, the knockdown of ETHE1 resulted in a decrease in the number of cells in the S phase, an increase in the number of cells in the G_1 phase, and no significant effect on the number of cells in the G_2 phase. In addition, the proportion of cells in the sub-G_1 phases suggested the occurrence of apoptosis. Western blot analysis showed that ETHE1 knockdown reduced the expression levels of cyclin D1 and CDK4 (Fig. 3E).

ETHE1 knockdown promotes GAC cell apoptosis. Apoptosis was further measured using Annexin V-PI staining combined with flow cytometry. As shown in Fig. 4A, compared with

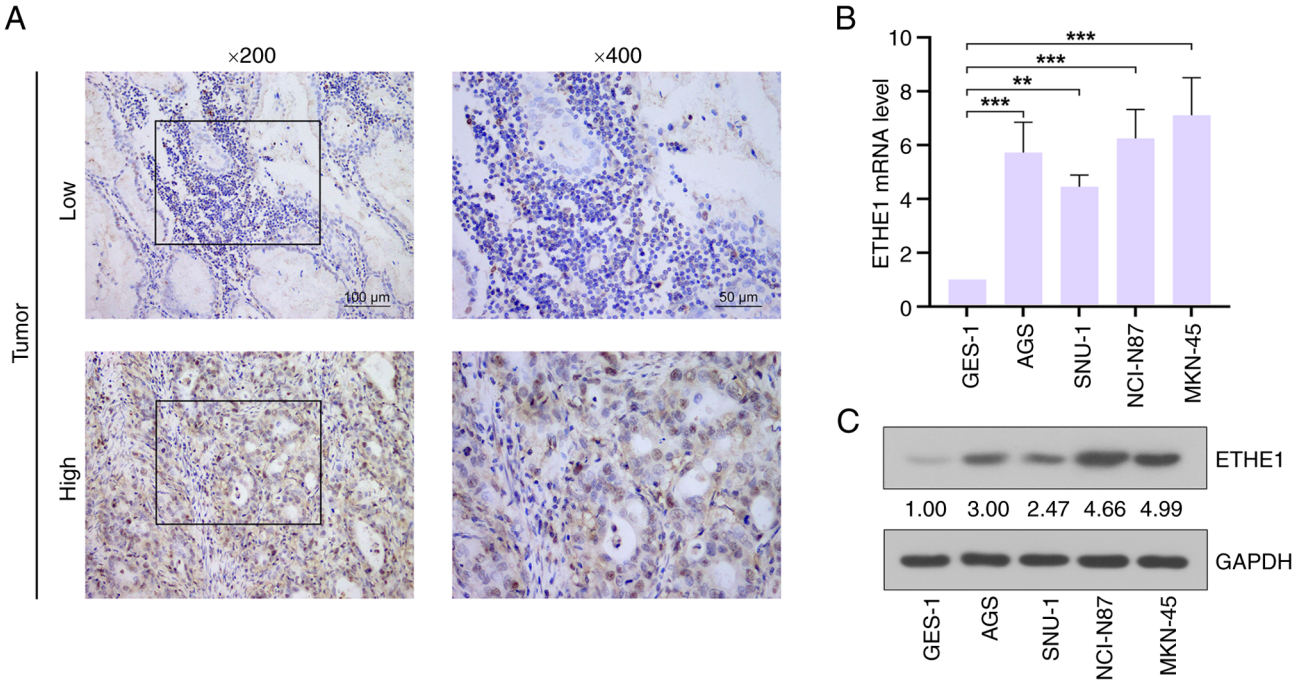

Figure 2. Expression of ETHE1 in tissues from patients with GAC and GAC cell lines. (A) Representative images of ETHE1 immunohistochemical staining in GAC tissue. Scale bar, 100 μm (magnification, x200); 50 μm (magnification, x400). (B) Reverse transcription-quantitative PCR and (C) western blotting of ETHEI expression in GAC cells. **P<0.01, ***P<0.001. ETHEI, ethylmalonic encephalopathy protein 1; GAC, gastric adenocarcinoma.

in the control group, knockdown of ETHE1 increased the proportion of apoptotic GAC cells. TUNEL staining also showed that ETHE1 knockdown promoted apoptosis (Fig. 4B). Further analysis of apoptosis-related enzyme activity revealed that knockdown of ETHE1 resulted in an increase in caspase-3 and caspase-9 activity (Fig. 4C and D).

ETHE1 knockdown inhibits aerobic glycolysis in GAC cells. Compared with in the control groups, knockdown of ETHE1 reduced glucose consumption, lactic acid production and ATP levels in GAC cells, as measured by the markers of glycolysis in GAC cells (Fig. 5A-C). In addition, knockdown of ETHE1 reduced the expression levels of glycolysis-related molecules, including glucose transporter type 1 (GLUT1), lactate dehydrogenase A (LDHA), hexokinase 2 (HK2) and pyruvate kinase isozyme type M2 (PKM2) (Fig. 5D).

ETHE1 downregulation inhibits tumor growth in vivo. The growth rate of tumors in the sh$^{708\text{-}728}$ group was lower than that in the control group *in vivo* (Fig. 6A). Starting from day 16, the tumor volume in the sh$^{708\text{-}728}$ group was smaller than that in the control group. The tumor weight of the sh$^{708\text{-}728}$ group was also lower than that of the control group. Compared with in the control group, Ki67 and ETHE1 expression in the tumor tissues of the sh$^{708\text{-}728}$ group was reduced (Fig. 6B), whereas apoptosis was increased (Fig. 6C).

ETHE1 is an important immunomodulator. To further explore the value of ETHE1 in immune regulation, the correlation between its expression and immunomodulator expression was analyzed in STAD. The expression of ETHE1 in STAD clinical samples was significantly positively correlated with immunosuppressive factors, such as galectin 9 (LGALS9), nectin cell adhesion molecule 2 (PVRL2), IL-10 receptor subunit β, CD274 and indoleamine 2,3-dioxygenase 1 (IDO1) (Fig. 7A). A negative correlation was identified between ETHE1 expression and immune-promoting factors, such as IL-6 receptor (IL6R), CD160, UL16 binding protein 1 (ULBP1), CD276 and CD40 (Fig. 7B). ETHE1 expression was also positively correlated with chemokines, such as C-X-C motif chemokine ligand (CXCL)5, CXCL3, CXCL16, CXCL1 and CXCL2 (Fig. 7C). These findings suggested that ETHE1 may contribute to the development of STAD. Although some correlations were not very strong (r value <0.3), they were still statistically significant, thus indicating that ETHE1 may be involved in the regulation of the expression of immune regulatory factors. In addition, compared with in the normal samples (paracancerous tissues, n=36), ETHE1 expression was upregulated in Tregs and M2 macrophages in STAD tumor tissues (n=414), suggesting that ETHE1 expression may mediate the malignant behavior of STAD (Fig. 7D).

Discussion

The high prevalence and mortality rate of GAC highlights a need to investigate the underlying molecular mechanisms. The results of the clinical sample analysis in the present study showed that ETHE1 expression was upregulated in GAC tissues, which was supported by the pan-cancer analysis from TCGA and GTEx, as well as ETHE1 expression in samples from the HPA. ETHE1 expression was associated with tumor stage, lymph node metastasis and TNM stage. Therefore, high ETHE1 expression may be predictive of a worse survival time, and it may serve a role in the pathogenesis and progression of GAC. Therefore, the regulation of tumorigenic behaviors by ETHE1 in GAC cells was assessed in the present study.

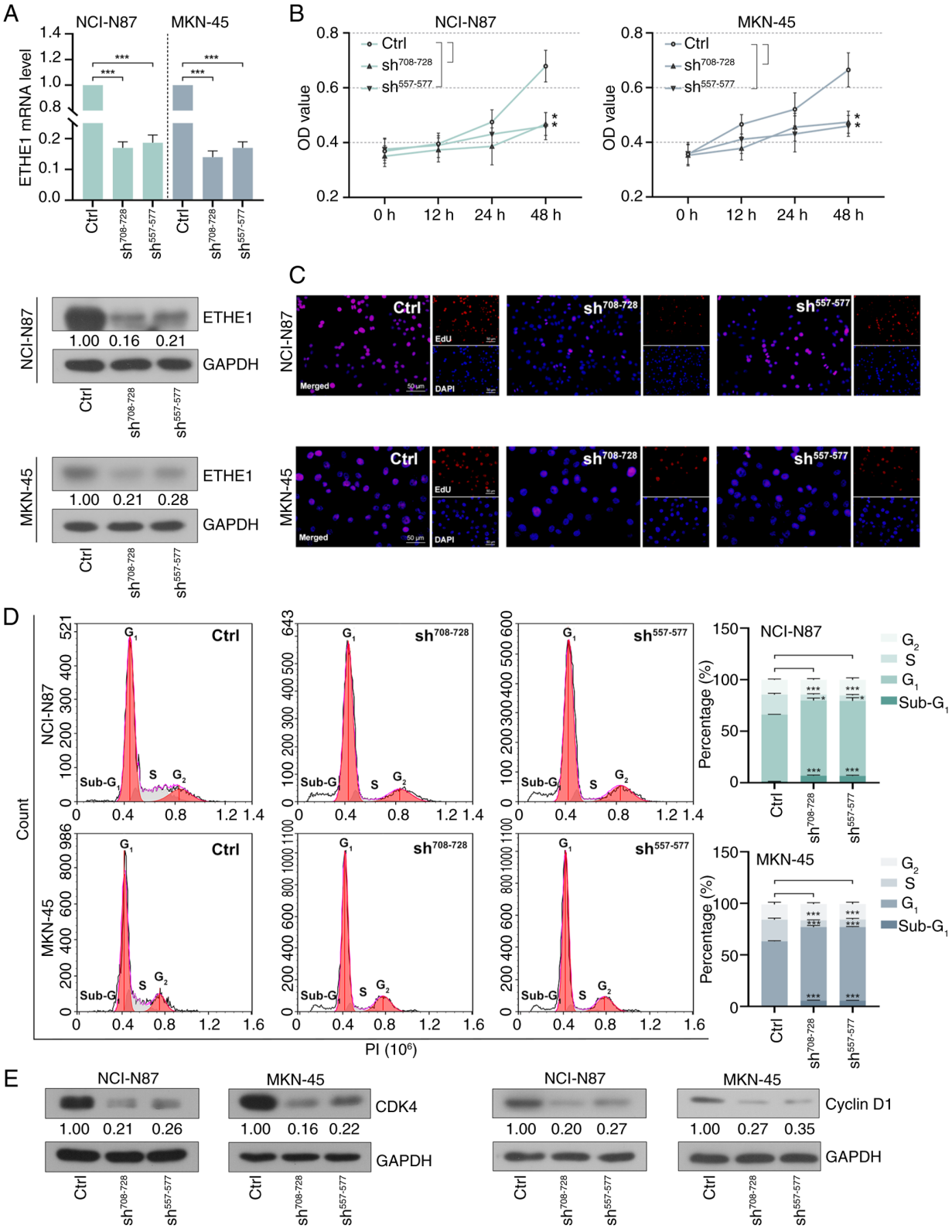

Figure 3. ETHE1 knockdown inhibits CAG cell proliferation. NCI-N87 and MKN-45 cells were infected with a lentivirus carrying ETHE1-specific shRNAs or a shRNA without any target sequence. (A) Reverse transcription-quantitative PCR and western blotting of ETHEI expression in gastric adenocarcinoma cells. (B) Cell proliferation during 48 h was detected using the Cell Counting Kit-8 assay. (C) Representative EdU staining images. Scale bar, 50 μm. (D) Flow cytometric analysis of cell cycle progression. (E) Western blot analysis of CDK4 and cyclin D1. *P<0.05, **P<0.01, **P<0.01 and ***P<0.001 vs. Ctrl or as indicated. CDK4, cyclin-dependent kinase 4; Ctrl, control; ETHEI, ethylmalonic encephalopathy protein 1; sh, short hairpin.

Compared with in control cells, ETHE1 knockdown reduced cyclin D1 and CDK4 levels in GAC cells. This resulted in a decrease in the number of cells in the S phase and an increase in the number of cells in the G_1 phase, ultimately inhibiting the proliferation of GAC cells. It has previously been reported that ETHE1 deficiency does not affect the cell cycle of fibroblasts,

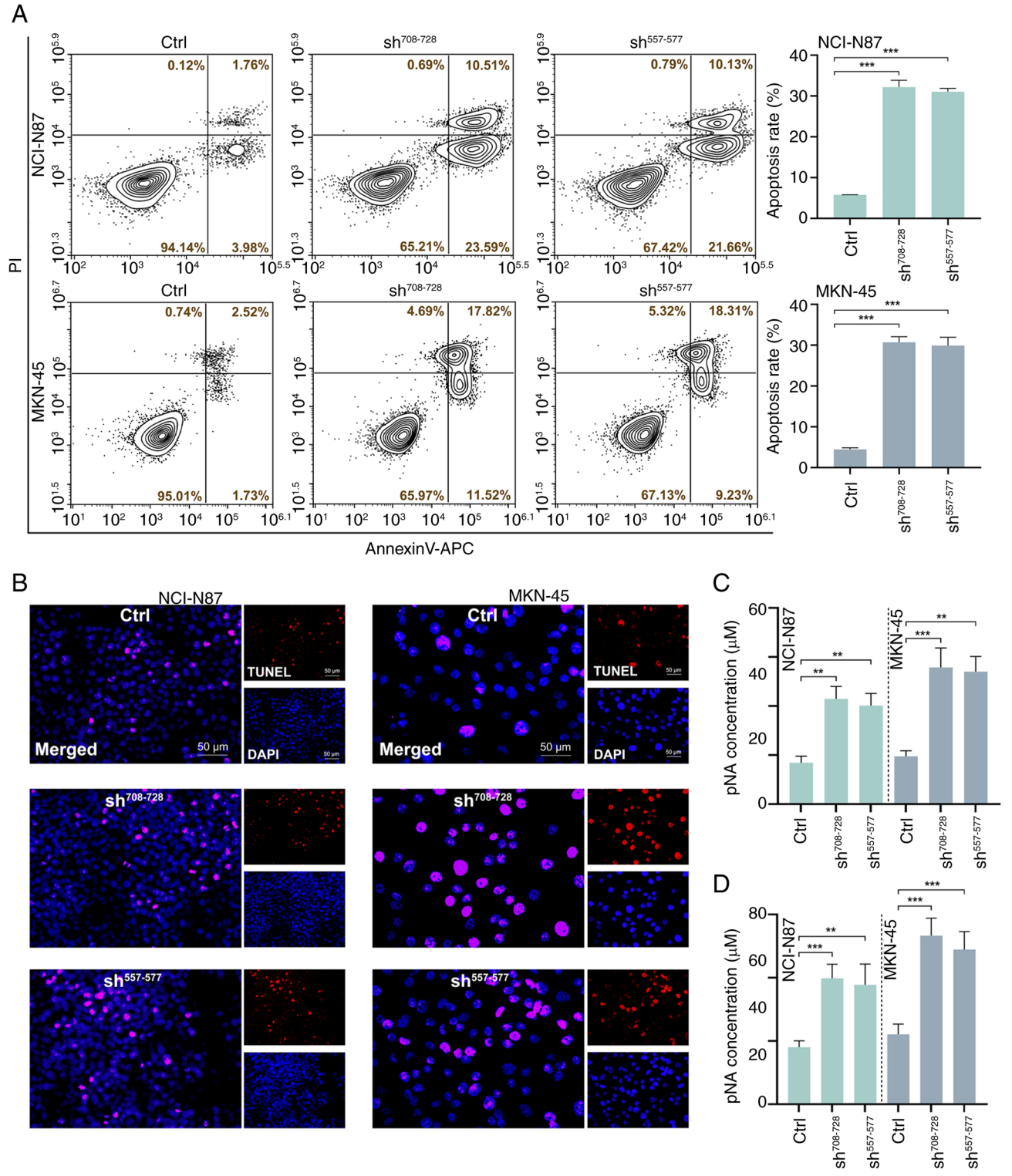

Figure 4. ETHE1 knockdown promotes CAG cell apoptosis. (A) Flow cytometric analysis of apoptosis. (B) Apoptosis of gastric adenocarcinoma cells was detected by TUNEL staining. Scale bar, 50 μm. (C) Caspase-3 and (D) caspase-9 activity was detected using kits. **P<0.01, ***P<0.001. Ctrl, control; sh, short hairpin.

which may be attributed to differences in cell types and the specific molecular mechanisms (17). It has also been suggested that ETHE1 serves a distinct role in tumor cells compared with in normal cells (15) . In the present study, in GAC, ETHE1 was shown to exhibit a pronounced effect in promoting cell proliferation, which is worthy of further attention. In contrast to cell proliferation, inducing apoptosis is an effective means of preventing cancer progression (24). It has previously been reported that overexpression of ETHE1 can inhibit the apoptosis of hepatoma cells (25). In the present study, knockdown of ETHE1 significantly enhanced caspase-3 and caspase-9 activity, thereby promoting the apoptosis of GAC cells.

The present study showed that knockdown of ETHE1 reduced proliferation and enhanced apoptosis of GAC cells,

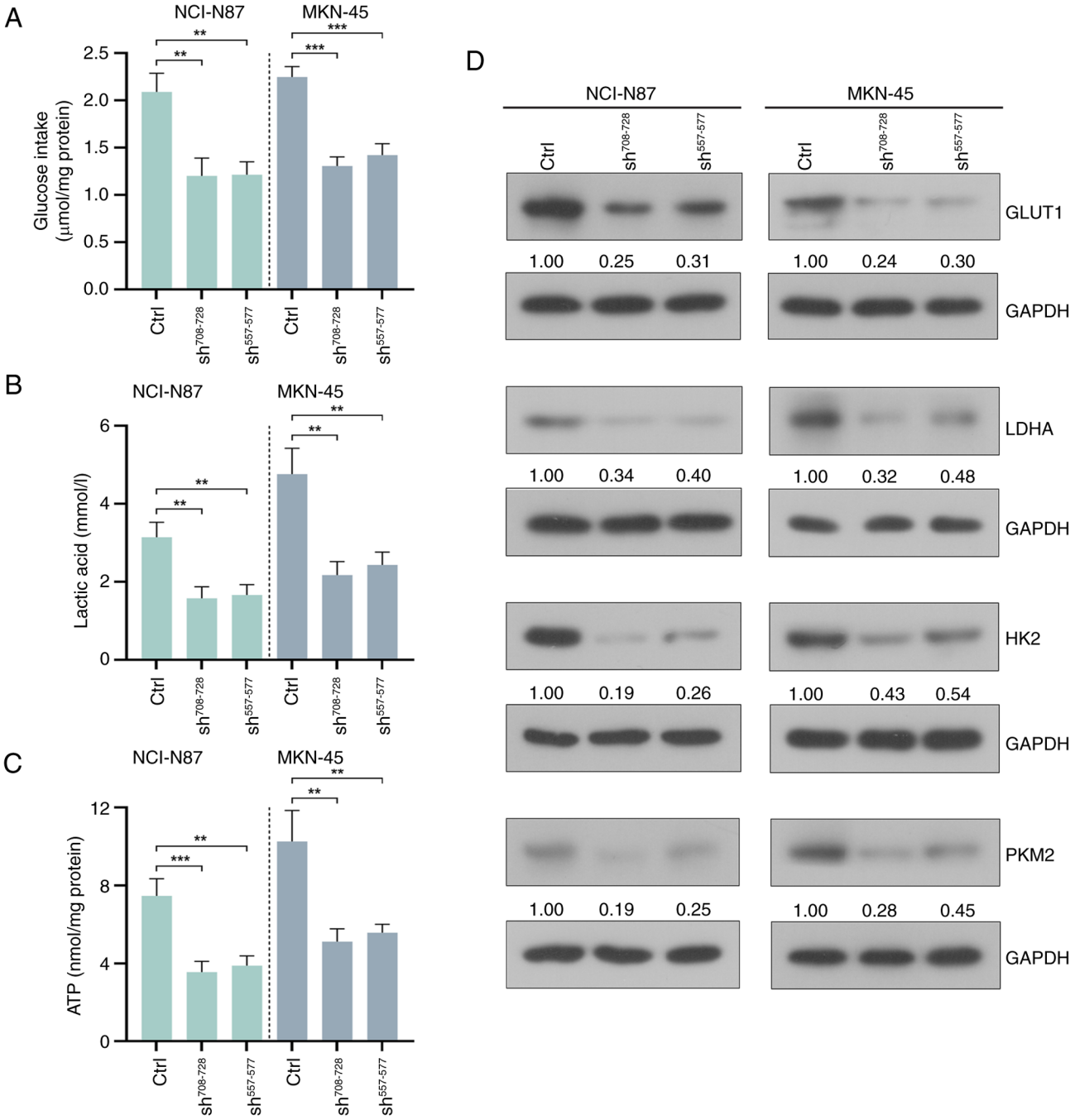

Figure 5. ETHE1 knockdown inhibits aerobic glycolysis in CAG cells. (A) Glucose consumption, (B) lactic acid production and (C) ATP levels were detected using kits. (D) Western blot analysis of GLUT1, LDHA, HK2 and PKM2. **P<0.01, ***P<0.001. Ctrl, control; GLUT1, glucose transporter type 1; LDHA, lactate dehydrogenase A; HK2, hexokinase 2; PKM2, pyruvate kinase isozyme type M2; sh, short hairpin.

indicating that ETHE1 expression may promote the development of GAC. Multiple studies have shown that ETHE1 is a mitochondrial protein involved in regulating mitochondrial dynamics. Impaired mitochondrial respiration in ethylmalonic encephalopathy is induced by a mutation in the ETHE1 gene, and ETHE1-deficient mice induced by acute depleted uranium have been shown to exhibit severe mitochondrial dysfunction (16). In a previous study, the mitochondrial protein expression profile of patients with ETHE1 deficiency was shown to be altered, primarily involving pathways such as oxidative phosphorylation and pyruvate metabolism (26), which may be closely related to the tumor microenvironment (TME). Increased glycolysis in cancer cells and the resulting high-lactic acid environment promote tumor growth (27-29). Previous studies have shown that upregulated expression of ETHE1 increases aerobic glycolysis in colorectal cancer cell lines, driving the growth of colorectal cancer tumors (15). In the present study, the expression of GLUT1, LDHA, HK2 and PKM2, and the content of glycolytic substrates and glycolytic products were determined. ETHE1 knockdown reduced the levels of glycolytic markers, the consumption of glucose, and the production of lactic acid and ATP. These results suggested that the knockdown of ETHE1 prevented glucose uptake and aerobic glycolysis in GAC cells; this may have

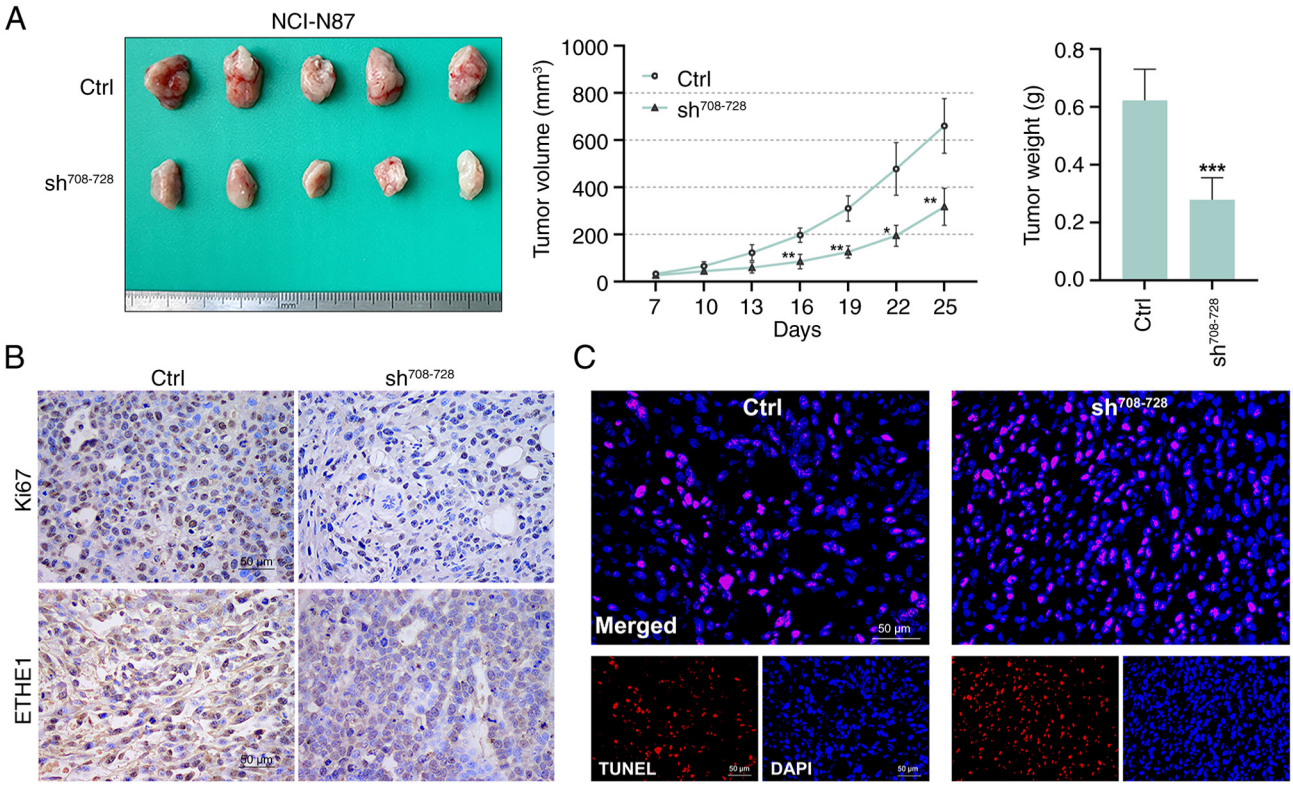

Figure 6. BALB/c nude mice received subcutaneous injections of stabilized infected NCI-N87 cells to induce tumor formation *in vivo*. (A) Tumor tissue images, tumor growth curve and tumor weight. (B) Representative immunohistochemical staining images of Ki67 and ETHE1. (C) Apoptosis in gastric adenocarcinoma tissue was detected by TUNEL staining. Scale bar, 100 μm. *P<0.05, **P<0.01 and ***P<0.001 vs. Ctrl. Ctrl, control; ETHEI, ethylmalonic encephalopathy protein 1; sh, short hairpin.

reduced the energy supply to GAC cells and restrained tumor growth. ETHE1 knockdown also suppressed tumor growth *in vivo*. Taken together, it was shown that ETHE1 may be a key factor in regulating aerobic glycolysis in GAC cells, and ETHE1 knockdown effectively inhibited GAC glycolysis, in turn reducing tumor proliferation and increasing tumor cell apoptosis.

Analysis of data from the TISIDB database revealed that the expression of ETHE1 was correlated with the expression of multiple immunomodulatory genes. LGALS9 is a pro-survival factor that induces immune escape by inhibiting immune responses controlled by T and NK cells (30). PVRL2 also inhibits anti-tumor immunity led by T cells NK cells (31). IL10RB is a receptor for IL-10, that mediates the inhibition of IL-10 on the antigen presentation of monocytes (32). CD274 (PD-L1) is a key immune checkpoint protein that binds to PD-1 on T cells, leading to tumor immune escape (33). IDO1 catalyzes the production of kynurenine, an agonist of the endogenous aryl hydrocarbon receptor, activating it, and contributing to immunosuppression and tumor immune escape (34). ETHE1 expression was positively correlated with the aforementioned immunosuppressive factors, suggesting the potential role of ETHE1 in tumor development.

IL-6 promotes T-cell proliferation after stimulation by T-cell receptors, and IL6R is a receptor that mediates IL-6 signal transduction (35). CD160 is an important NK cell-activating receptor that is expressed in $CD8^{+}$T cells (36,37). Notably, there has been reported to be an increase in $CD160^{+}$ cells in the tumor tissues of patients with GC undergoing immunotherapy (38). ULBP1 is a ligand of the killer cell lectin like receptor k1 receptor, and the malignant phenotype of GC cells is enhanced following ULBP1 downregulation (39). CD276 (B7-H3) induces T-cell proliferation and IFN-γ production through a non-costimulatory pathway, and CD276 has been shown to be positively associated with the prognosis of patients with GC (40). CD40 is a member of the tumor necrosis factor receptor superfamily and is widely expressed in immune cells (41); activation of CD40 allows dendritic cells to promote T-cell activation and induces macrophages to destroy the tumor matrix (42). Notably, in the present study ETHE1 expression was negatively correlated with these immune-promoting factors, suggesting that targeting ETHE1 may promote antitumor immunity.

Chemokines bind to their cell surface receptors in immune responses, thereby promoting receptor internalization and signaling (43). The receptor of CXCL5, CXCL3, CXCL1 and CXCL2 is C-X-C motif chemokine receptor (CXCR)1, and the receptor of CXCL16 is CXCR6. Notably, activation of CXCR1 and CXCR6 can promote the malignant phenotype of GC cells (44,45). In the current study, ETHE1 expression was positively correlated with CXCL5, CXCL3, CXCL1, CXCL2 and CXCL16, suggesting that the molecular mechanisms involved in ETHE1-induced GAC development may involve chemokine signaling pathways.

Tregs are important sources of immunosuppressive factors. In the TME, Tregs are induced to differentiate by conventional T cells; they inhibit antitumor immunity and thus promote

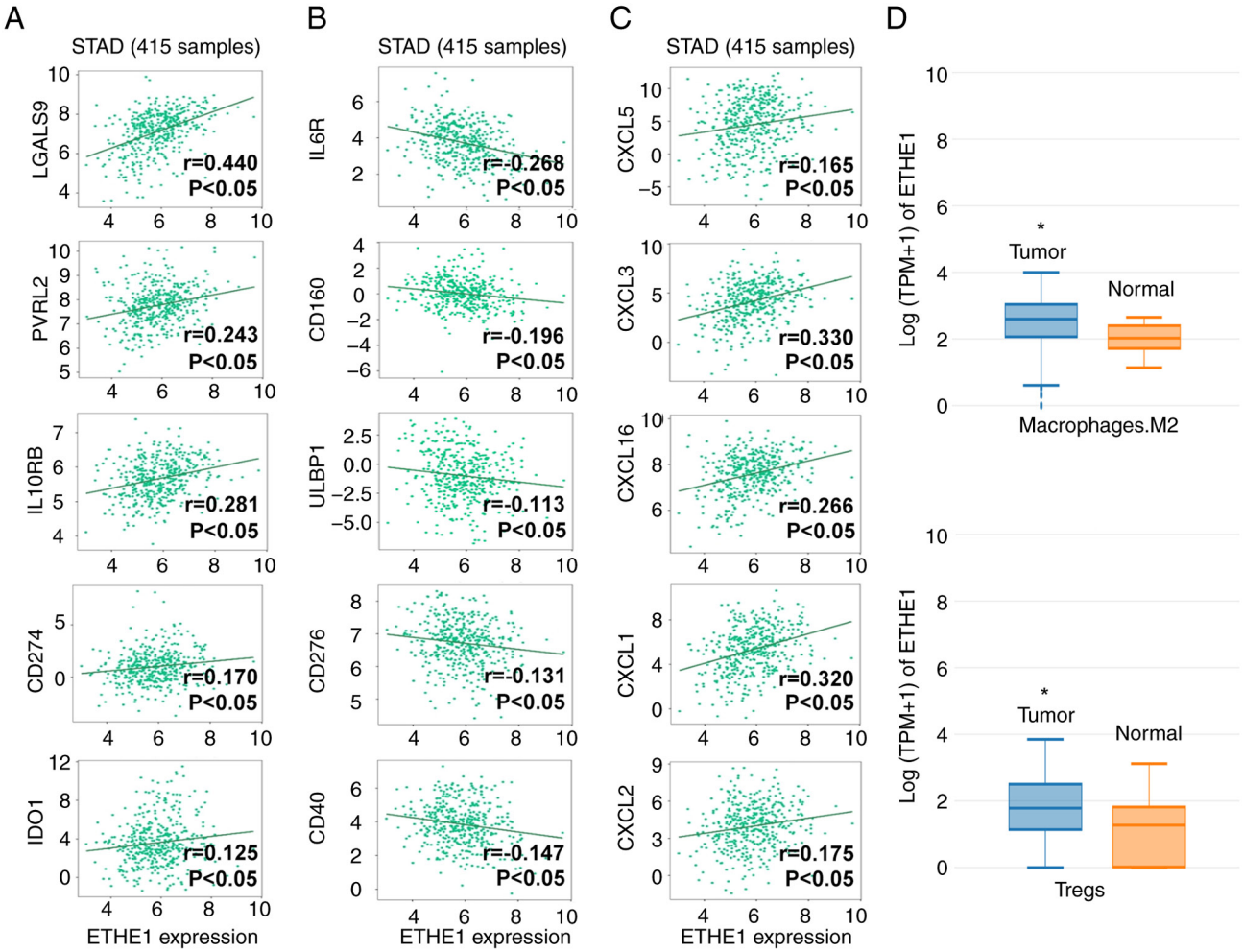

Figure 7. Analysis of ETHE1 expression in immune regulation of STAD. Correlation analysis of ETHE1 with (A) immunosuppressive factors, (B) immune-promoting factors and (C) chemokines in STAD using the TISIDB database. (D) Expression of ETHE1 in M2 macrophages and Tregs in STAD tissues from using Gene Expression Profiling Interactive Analysis database. *P<0.05 vs. Normal. CXCL, C-X-C motif chemokine ligand; ETHEI, ethylmalonic encephalopathy protein 1; IDO1, indoleamine 2,3-dioxygenase 1; IL6R, IL-6 receptor; IL10RB, IL-10 receptor subunit β; LGALS9, galectin 9; PVRL2, nectin cell adhesion molecule 2; STAD, stomach adenocarcinoma; Tregs, regulatory T cells; ULBP1, UL16 binding protein 1.

tumor development (46). Furthermore, increased Treg infiltration is associated with a poor prognosis in patients with GC (47). Macrophages are the most abundant population of innate immune cells recruited to tumor immune sites, and they tend to be more polarized toward the M2 phenotype in the TME (48). In addition, patients with GC with low levels of infiltration of M2 macrophages have a better prognosis (49). Through analysis of data obtained from TCGA using the GEPIA database, it was revealed that the expression of ETHE1 in Tregs and M2 macrophages in STAD was significantly higher than that in Tregs and M2 macrophages in normal tissues. Thus, targeting ETHE1 alongside immunotherapy may improve outcomes for patients with GC.

The results of the present study indicated that ETHE1 expression was upregulated in GAC tissues. Furthermore, its expression levels showed a positive association with tumor stage, lymph node metastasis and TNM classification. Knockdown of ETHE1 inhibited the GAC glycolytic process, leading to the suppression of proliferation and the promotion of apoptosis of tumor cells *in vivo* and *in vitro*. The current study primarily focused on the effect of ETHE1 on tumor growth in GAC, but ETHE1 may not be limited to this. It has been reported that overexpression of ETHE1 promotes metastasis of triple-negative breast cancer, rather than tumor growth (14). ETHE1 may thus serve different roles in different types of cancer, and its role in GAC metastasis requires further exploration.

In conclusion, the knockdown of ETHE1 reduced tumor cell proliferation and promoted tumor cell apoptosis by inhibiting GAC cell aerobic glycolysis.

Acknowledgements

Not applicable.

Funding

This research was funded by the Beijing Medical Award Foundation (grant no. YXJL-2020-1152-0161).

Availability of data and materials

The data generated in the present study may be requested from the corresponding author.

Authors' contributions

FFL conceptualized the present study, designed and carried out the experiments, analyzed the data and wrote the original draft. XD designed and carried out the experiment, analyzed the data and wrote the original draft. MH and XYF carried out the experiments, analyzed the data, provided the materials and generated the figures. CMJ conceptualized the present study, reviewed and edited the manuscript, and supervised this work. MH and XYF confirm the authenticity of all the raw data. All authors read and approved the final version of the manuscript.

Ethics approval and consent to participate

All the specimens were collected under a protocol approved by the Ethics Committee of The Second Hospital of Dalian Medical University (2023; approval no. 136). Each patient participated after providing written informed consent. The study was performed in accordance with The Declaration of Helsinki. All animal experiments have been approved by the Animal Care and Welfare Committee of Dalian Medical University (approval no. AEE23074).

Patient consent for publication

Not applicable.

Competing interests

The authors declare that they have no competing interests.

References

1. Sung H, Ferlay J, Siegel RL, Laversanne M, Soerjomataram I, Jemal A and Bray F: Global cancer statistics 2020: GLOBOCAN estimates of incidence and mortality worldwide for 36 cancers in 185 countries. CA Cancer J Clin 71: 209-249, 2021.
2. Ramezankhani R, Solhi R, Es HA, Vosough M and Hassan M: Novel molecular targets in gastric adenocarcinoma. Pharmacol Ther 220: 107714, 2021.
3. Smyth EC, Nilsson M, Grabsch HI, van Grieken NC and Lordick F: Gastric cancer. Lancet 396: 635-648, 2020.
4. Ganapathy-Kanniappan S and Geschwind JF: Tumor glycolysis as a target for cancer therapy: Progress and prospects. Mol Cancer 12: 152, 2013.
5. Ngo DC, Ververis K, Tortorella SM and Karagiannis TC: Introduction to the molecular basis of cancer metabolism and the Warburg effect. Mol Biol Rep 42: 819-823, 2015.
6. Liberti MV and Locasale JW: The Warburg effect: How does it benefit cancer cells? Trends Biochem Sci 41: 211-218, 2016.
7. Huber V, Camisaschi C, Berzi A, Ferro S, Lugini L, Triulzi T, Tuccitto A, Tagliabue E, Castelli C and Rivoltini L: Cancer acidity: An ultimate frontier of tumor immune escape and a novel target of immunomodulation. Semin Cancer Biol 43: 74-89, 2017.
8. Dhup S, Dadhich RK, Porporato PE and Sonveaux P: Multiple biological activities of lactic acid in cancer: Influences on tumor growth, angiogenesis and metastasis. Curr Pharm Des 18: 1319-1330, 2012.
9. Ren Z, Rajani C and Jia W: The distinctive serum metabolomes of gastric, esophageal and colorectal cancers. Cancers (Basel) 13: 720, 2021.
10. Chan AW, Gill RS, Schiller D and Sawyer MB: Potential role of metabolomics in diagnosis and surveillance of gastric cancer. World J Gastroenterol 20: 12874-12882, 2014.
11. Han S, Yang S, Cai Z, Pan D, Li Z, Huang Z, Zhang P, Zhu H, Lei L and Wang W: Anti-Warburg effect of rosmarinic acid via miR-155 in gastric cancer cells. Drug Des Devel Ther 9: 2695-2703, 2015.
12. Wang YY, Zhou YQ, Xie JX, Zhang X, Wang SC, Li Q, Hu LP, Jiang SH, Yi SQ, Xu J, *et al*: MAOA suppresses the growth of gastric cancer by interacting with NDRG1 and regulating the Warburg effect through the PI3K/AKT/mTOR pathway. Cell Oncol (Dordr) 46: 1429-1444, 2023.
13. Holdorf MM, Owen HA, Lieber SR, Yuan L, Adams N, Dabney-Smith C and Makaroff CA: Arabidopsis ETHE1 encodes a sulfur dioxygenase that is essential for embryo and endosperm development. Plant Physiol 160: 226-236, 2012.
14. Yang SY, Liao L, Hu SY, Deng L, Andriani L, Zhang TM, Zhang YL, Ma XY, Zhang FL, Liu YY and Li DQ: ETHE1 accelerates triple-negative breast cancer metastasis by activating GCN2/eIF2α/ATF4 signaling. Int J Mol Sci 24: 14566, 2023.
15. Witherspoon M, Sandu D, Lu C, Wang K, Edwards R, Yeung A, Gelincik O, Manfredi G, Gross S, Kopelovich L and Lipkin S: ETHE1 overexpression promotes SIRT1 and PGC1α mediated aerobic glycolysis, oxidative phosphorylation, mitochondrial biogenesis and colorectal cancer. Oncotarget 10: 4004-4017, 2019.
16. Liu S, Wang S, Zhao Y, Li J, Shu C, Li Y, Li J, Lu B, Xu Z, Ran Y and Hao Y: Depleted uranium causes renal mitochondrial dysfunction through the ETHE1/Nrf2 pathway. Chem Biol Interact 372: 110356, 2023.
17. Sahebekhtiari N, Fernandez-Guerra P, Nochi Z, Carlsen J, Bross P and Palmfeldt J: Deficiency of the mitochondrial sulfide regulator ETHE1 disturbs cell growth, glutathione level and causes proteome alterations outside mitochondria. Biochim Biophys Acta Mol Basis Dis 1865: 126-135, 2019.
18. Oue N, Hamai Y, Mitani Y, Matsumura S, Oshimo Y, Aung PP, Kuraoka K, Nakayama H and Yasui W: Gene expression profile of gastric carcinoma: Identification of genes and tags potentially involved in invasion, metastasis, and carcinogenesis by serial analysis of gene expression. Cancer Res 64: 2397-2405, 2004.
19. Yasui W, Oue N, Ito R, Kuraoka K and Nakayama H: Search for new biomarkers of gastric cancer through serial analysis of gene expression and its clinical implications. Cancer Sci 95: 385-392, 2004.
20. Tang Z, Li C, Kang B, Gao G, Li C and Zhang Z: GEPIA: A web server for cancer and normal gene expression profiling and interactive analyses. Nucleic Acids Res 45: W98-W102, 2017.
21. Ru B, Wong CN, Tong Y, Zhong JY, Zhong SSW, Wu WC, Chu KC, Wong CY, Lau CY, Chen I, *et al*: TISIDB: An integrated repository portal for tumor-immune system interactions. Bioinformatics 35: 4200-4202, 2019.
22. Guidelines for Endpoints in Animal Study Proposals. Animal Research Advisory Committee NIH (ed.).
23. Livak KJ and Schmittgen TD: Analysis of relative gene expression data using real-time quantitative PCR and the 2(-Delta Delta C(T)) method. Methods 25: 402-408, 2001.
24. Gong Y, Fan Z, Luo G, Yang C, Huang Q, Fan K, Cheng H, Jin K, Ni Q, Yu X and Liu C: The role of necroptosis in cancer biology and therapy. Mol Cancer 18: 100, 2019.
25. Higashitsuji H, Higashitsuji H, Nagao T, Nonoguchi K, Fujii S, Itoh K and Fujita J: A novel protein overexpressed in hepatoma accelerates export of NF-kappa B from the nucleus and inhibits p53-dependent apoptosis. Cancer Cell 2: 335-346, 2002.
26. Sathe G, Deepha S, Gayathri N, Nagappa M, Sankaran BP, Taly AB, Khanna T, Pandey A and Govindaraj P: Ethylmalonic encephalopathy ETHE1 p. D165H mutation alters the mitochondrial function in human skeletal muscle proteome. Mitochondrion 58: 64-71, 2021.
27. Watson MJ, Vignali PDA, Mullett SJ, Overacre-Delgoffe AE, Peralta RM, Grebinoski S, Menk AV, Rittenhouse NL, DePeaux K, Whetstone RD, *et al*: Metabolic support of tumour-infiltrating regulatory T cells by lactic acid. Nature 591: 645-651, 2021.
28. Brand A, Singer K, Koehl GE, Kolitzus M, Schoenhammer G, Thiel A, Matos C, Bruss C, Klobuch S, Peter K, *et al*: LDHA-Associated lactic acid production blunts tumor immunosurveillance by T and NK cells. Cell Metab 24: 657-671, 2016.
29. Sonveaux P, Végran F, Schroeder T, Wergin MC, Verrax J, Rabbani ZN, De Saedeleer CJ, Kennedy KM, Diepart C, Jordan BF, *et al*: Targeting lactate-fueled respiration selectively kills hypoxic tumor cells in mice. J Clin Invest 118: 3930-3942, 2008.
30. Yıldırım C: Galectin-9, a pro-survival factor inducing immunosuppression, leukemic cell transformation and expansion. Mol Biol Rep 51: 571, 2024.

31. Murakami K and Ganguly S: The Nectin family ligands, PVRL2 and PVR, in cancer immunology and immunotherapy. Front Immunol 15: 1441730, 2024.
32. Saraiva M, Vieira P and O'Garra A: Biology and therapeutic potential of interleukin-10. J Exp Med 217: e20190418, 2020.
33. Gou Q, Dong C, Xu H, Khan B, Jin J, Liu Q, Shi J and Hou Y: PD-L1 degradation pathway and immunotherapy for cancer. Cell Death Dis 11: 955, 2020.
34. Cheong JE and Sun L: Targeting the IDO1/TDO2-KYN-AhR pathway for cancer immunotherapy-challenges and opportunities. Trends Pharmacol Sci 39: 307-325, 2018.
35. Fisher DT, Appenheimer MM and Evans SS: The two faces of IL-6 in the tumor microenvironment. Semin Immunol 26: 38-47, 2014.
36. Zhang L, Zhang A, Zhu X, Tian X, Guo J, He Q, Zhu L, Yuan S, Zhao C, Zhang X and Xu J: CD160 signaling is essential for CD8+ T cell memory formation via upregulation of 4-1BB. J Immunol 211: 1367-1375, 2023.
37. Le Bouteiller P, Tabiasco J, Polgar B, Kozma N, Giustiniani J, Siewiera J, Berrebi A, Aguerre-Girr M, Bensussan A and Jabrane-Ferrat N: CD160: A unique activating NK cell receptor. Immunol Lett 138: 93-96, 2011.
38. Wang J, Liang Y, Xue A, Xiao J, Zhao X, Cao S, Li P, Dong J, Li Y, Xu Z and Yang L: Intratumoral CXCL13(+) CD160(+) CD8(+) T cells promote the formation of tertiary lymphoid structures to enhance the efficacy of immunotherapy in advanced gastric cancer. J Immunother Cancer 12: e009603, 2024.
39. Hu B, Tian X, Li Y, Liu Y, Yang T, Han Z, An J, Kong L and Li Y: Epithelial-mesenchymal transition may be involved in the immune evasion of circulating gastric tumor cells via downregulation of ULBP1. Cancer Med 9: 2686-2697, 2020.
40. Wu CP, Jiang JT, Tan M, Zhu YB, Ji M, Xu KF, Zhao JM, Zhang GB and Zhang X: Relationship between co-stimulatory molecule B7-H3 expression and gastric carcinoma histology and prognosis. World J Gastroenterol 12: 457-459, 2006.
41. Guo J, Xiao JJ, Zhang X and Fan KX: CD40 expression and its prognostic significance in human gastric carcinoma. Med Oncol 32: 63, 2015.
42. Vonderheide RH: CD40 agonist antibodies in cancer immunotherapy. Annu Rev Med 71: 47-58, 2020.
43. Balkwill FR: The chemokine system and cancer. J Pathol 226: 148-157, 2012.
44. Wang J, Hu W, Wu X, Wang K, Yu J, Luo B, Luo G, Wang W, Wang H, Li J and Wen J: CXCR1 promotes malignant behavior of gastric cancer cells in vitro and in vivo in AKT and ERK1/2 phosphorylation. Int J Oncol 48: 2184-2196, 2016.
45. Han J, Fu R, Chen C, Cheng X, Guo T, Huangfu L, Li X, Du H, Xing X and Ji J: CXCL16 promotes gastric cancer tumorigenesis via ADAM10-Dependent CXCL16/CXCR6 axis and activates akt and mapk signaling pathways. Int J Biol Sci 17: 2841-2852, 2021.
46. Li C, Jiang P, Wei S, Xu X and Wang J: Regulatory T cells in tumor microenvironment: New mechanisms, potential therapeutic strategies and future prospects. Mol Cancer 19: 116, 2020.
47. Qu Y, Wang X, Bai S, Niu L, Zhao G, Yao Y, Li B and Li H: The effects of TNF-α/TNFR2 in regulatory T cells on the microenvironment and progression of gastric cancer. Int J Cancer 150: 1373-1391, 2022.
48. Zhang Q and Sioud M: Tumor-associated macrophage subsets: Shaping polarization and targeting. Int J Mol Sci 24: 7493, 2023.
49. Wu Y, Hao Y, Zhuang Q, Ma X and Shi C: AKR1B10 regulates M2 macrophage polarization to promote the malignant phenotype of gastric cancer. Biosci Rep 43: BSR20222007, 2023.